Front. Chem. Sci. Eng. 2025, 19(6): 46
https://doi.org/10.1007/s11705-025-2547-0

REVIEW ARTICLE

A review on the low temperature water-gas-shift reaction: reaction mechanism, catalyst design, and novel process development

Jun Li, Xiaonan Wang, Sen Yao, Xiao Zhang (✉)

School of Chemistry, State Key Laboratory of Fine Chemicals, Dalian University of Technology, Dalian 116024, China

Abstract The water-gas shift (WGS) reaction plays a pivotal role in various industrial processes, particularly in hydrogen production and carbon monoxide removal. As global energy demands rise and environmental concerns intensify, the development of efficient and sustainable catalysts for the low-temperature WGS (LT-WGS) reaction has gained significant attention. This review focuses on recent advancements in water-gas-shift catalyst design for low-temperature conditions and emerging renewable energy-driven catalytic processes, such as photocatalysis, electrocatalysis, and plasma catalysis for the WGS reaction, which are less commonly explored in existing reviews. We systematically analyze mechanisms studies of LT-WGS, rational catalyst design strategies, and recent frontier advances in the development of highly efficient catalysts. Furthermore, this review provides actionable insights for refining catalyst architectures, enhancing operational efficiency, elucidating reaction pathways, and pioneering hybrid technologies, all contributing to further advancements in this field.

Keywords water gas shift, hydrogen production, supported catalysts, reaction mechanism, innovative reaction processes

1 Introduction

The overreliance on conventional fossil fuels, such as oil, natural gas, and coal, has accelerated environmental degradation and climate instability [1]. As global economic growth intensifies, the escalating demand for these finite resources starkly contrasts with their rapidly diminishing reserves, necessitating an urgent transition to sustainable alternatives. Hydrogen, a recognized clean energy source, produces only water vapor when combusted and does not emit carbon dioxide, greenhouse gases, or harmful pollutants, making it an attractive substitute for traditional fossil fuels [2]. Furthermore, hydrogen is abundant, renewable, and possesses high energy density, making it a promising candidate for diverse applications in industries, transportation, and construction [3].

Hydrogen exists in water, hydrocarbons, biomass, and fossil fuels. Currently, the predominant methods for hydrogen production include fossil fuel-based hydrogen production, biomass gasification, water electrolysis, and other emerging technologies [4]. Fossil fuel-based hydrogen production, primarily through steam reforming of hydrocarbons, accounts for over 92% of global hydrogen production [5]. Despite its dominance, this process generates significant amounts of CO, which can poison catalysts, hindering the efficiency of hydrogen production and limiting its applications, particularly in fuel cells [6]. Biomass gasification is a renewable technology with energy-saving potential, but it suffers from low hydrogen production rates, high energy consumption, and the potential generation of tar, which complicates its industrial use [7]. While theoretically promising for high-purity hydrogen, conventional electrolysis remains constrained by excessive electrical energy inputs and prohibitive operational costs [8].

The most prevalent method of hydrogen production remains the steam reforming of hydrocarbons, but the CO generated during this process poses significant challenges. The water-gas shift (WGS) reaction is a critical technology for mitigating this issue. By converting CO and water into CO_2 and hydrogen, the WGS reaction not only removes harmful CO but also improves the purity of the hydrogen produced, enabling its use in sensitive applications like fuel cells and

Received January 21, 2025; accepted March 12, 2025;
online April 15, 2025

E-mail: zhangxiao@dlut.edu.cn

ammonia synthesis [6,9−11]. This makes WGS an indispensable process in hydrogen production systems that require high-purity hydrogen.

In addition to its role in traditional hydrogen production, the WGS reaction is crucial in emerging *in situ* hydrogen production technologies, such as alcohol reforming [12]. Organic liquid fuels, including methanol, ethanol, dimethyl ether, and glycerol, are commonly reformed to produce hydrogen [13−15]. However, these processes inevitably generate CO, making the *in situ* removal of CO a key challenge. The WGS reaction's capacity to simultaneously purify hydrogen streams and reduce CO levels on-site is indispensable for enhancing both the efficiency and practical viability of these systems, especially in sensitive applications like hydrogen fuel cells [16].

Given the increasing demand for cleaner and more efficient hydrogen production, the development of LT-WGS catalysts has become a central area of research. These catalysts play a vital role in improving the efficiency of hydrogen production by enabling CO removal at lower temperatures, which is particularly important for emerging technologies.

Here, we emphasize our unique focus on catalyst design and reaction mechanisms for LT-WGS reactions and the integration of renewable energy sources for driving these reactions. This approach distinguishes our review from previous reviews that predominantly address conventional catalytic systems and reaction mechanisms, thereby providing a novel perspective on the latest advancements in the field [17−22]. Specially, this article provides an overview of the progress made in the development of LT-WGS catalysts, with a focus on different types of supports, catalyst interface structures, active sites, reactant adsorption, and reaction mechanisms. The article explores catalysts ranging from reducible and non-reducible supports to novel materials such as transition metal carbon/nitride, carbon-based, and reverse interface structure metal supports. Furthermore, it highlights alternative WGS methods, including electrocatalytic, photocatalytic, and plasma-driven processes. These innovative approaches offer solutions to the limitations of traditional thermal catalysis, presenting more sustainable and efficient pathways for the future of WGS reactions (Fig. 1).

2 The thermodynamics, kinetics, and mechanism for the WGS reaction

WGS is a chemical reaction process in which CO is combined with water vapor to form CO_2 and H_2. The reaction equation is expressed as follows: CO (g) + H_2O (g) → CO_2 (g) + H_2 (g) (ΔH_r^θ = –41.09 kJ·mol^{-1}). The WGS reaction was first proposed by the Italian scientist Felice Fontana in 1780 [26]. In 1888, Mond and Langer were granted the first patent, applying it as a method to enrich hydrogen for fuel cell applications [27]. In 1915, the WGS reaction was first applied on an industrial scale

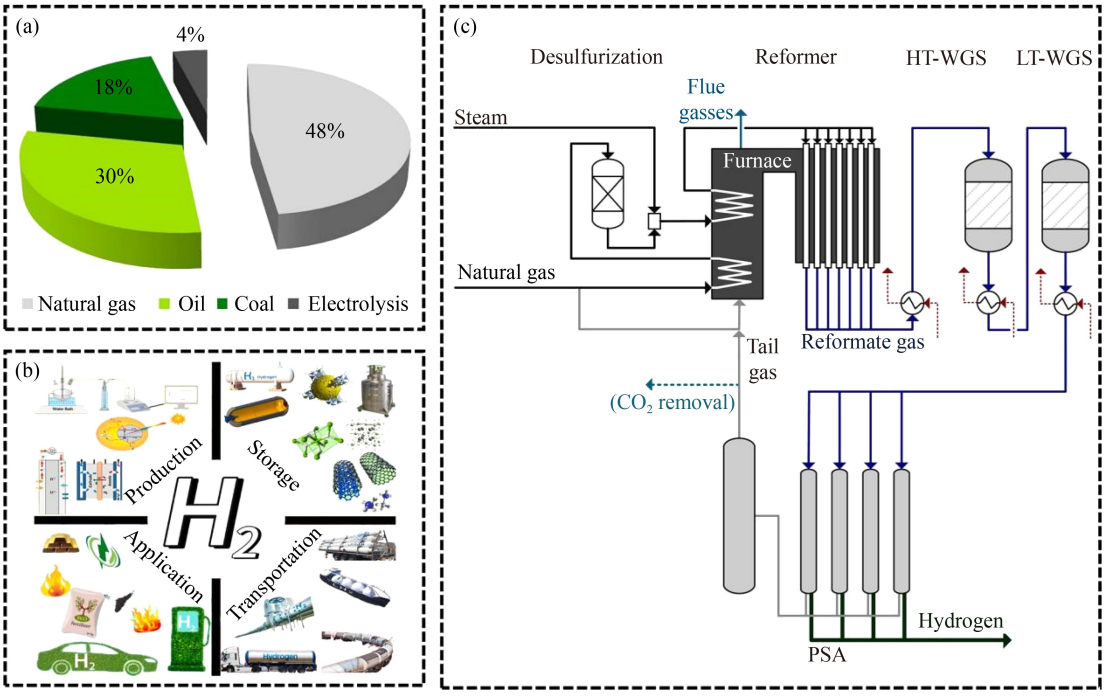

Fig. 1 (a) Distribution of current hydrogen sources. Reprinted with permission from Ref. [23], copyright 2018, Elsevier. (b) Hydrogen production pathways and hydrogen applications. Reprinted with permission from Ref. [24], copyright 2024, Elsevier. (c) Simplified process flow diagram for hydrogen production from natural gas steam reforming (HT-WGS: high-temperature WGS). Reprinted with permission from Ref. [25], copyright 2021, Elsevier.

in the Haber-Bosch ammonia synthesis process developed in Germany [28]. The industrial application of the WGS reaction has a history of over 90 years, with widespread applications in hydrogen production industries using coal, oil, and natural gas as raw materials, as well as in the ammonia synthesis industry. In the catalytic processes of syngas-to-methanol and syngas-to-hydrocarbons, LT-WGS are commonly used to remove large amounts of CO in methanol reforming for hydrogen production [29]. Furthermore, in daily life, it is also applied in areas such as automobile exhaust treatment and reducing CO content in domestic gas.

2.1 Thermodynamic of the WGS reaction

The WGS reaction is exothermic and reversible, thus low temperatures promote the equilibrium shift to the right, resulting in a higher CO conversion rate [19]. However, these thermodynamic advantages come at the cost of slower reaction kinetics at low temperatures, necessitating elevated temperatures to enhance the reaction rate [30]. To optimize both the thermodynamics and kinetics of the reaction and to achieve high catalytic conversion efficiency, WGS is commonly implemented in the industry using a multi-stage method, involving a combination of high-temperature and low-temperature reactions. The first stage is the HT-WGS reaction, with a reaction temperature range of 623–723 K and an outlet CO concentration of 3%–5%. The second stage is the LT-WGS, operating at a temperature range of 463–523 K, with an outlet CO concentration of approximately 0.3%, approaching the equilibrium conversion rate (Fig. 1(c)) [25].

From a thermodynamic perspective, according to the Gibbs free energy equation, $\Delta G = \Delta H - T\Delta S$, the reaction is an exothermic reaction, meaning that the system's free energy decreases, and the reaction occurs spontaneously, with the aim of achieving a lower energy state. As shown in Eq. (1) [31], in the WGS reaction, the equilibrium constant (K_p) is a function of temperature:

$$\ln(K_p) = \frac{5693.5}{T} + 1.077\ln(T) + 5.44\times10^{-4} - 1.125\times10^{-7}T^2 - \frac{49170}{T^2} - 13.148, \quad (1)$$

$$K_p = \frac{P_{CO_2}P_{H_2}}{P_{CO}P_{H_2O}}. \quad (2)$$

$P_{CO_2}, P_{CO}, P_{H_2}, P_{H_2O}$ are the types of gases designed in the WGS reaction respectively here [32].

At a given temperature and pressure, the value of the equilibrium constant determines whether the reaction favors the products more than the reactants. If K_p is greater than 1, the reaction proceeds in the forward direction. Conversely, if K_p is less than 1, the reaction goes in the reverse direction; and if K_p equals 1, the system is at equilibrium with equal concentrations of products and reactants. As shown in Fig. 2, increasing the molar ratio of steam to CO enhances the equilibrium conversion of CO, especially at temperatures above 423 K [33]. In addition, the thermodynamics of the WGS reaction can also be defined by Gibbs free energy, as shown in Eq. (3). The Gibbs free energy of the reaction increases with rising temperature and becomes positive around 1100 K, which suggests that higher temperatures make the reaction thermodynamically unfavorable [22].

$$\Delta G = -RT(\ln K_p). \quad (3)$$

2.2 Kinetics and mechanism of the WGS reaction

Numerous researchers have incorporated kinetic models in the study of the WGS reaction process, yet controversies regarding WGS kinetics have persisted over the years [34,35]. Understanding the reaction kinetics is crucial not only for catalyst design but also for gaining deeper insights into the reaction mechanism. The Langmuir-Hinshelwood model, a mechanistic framework widely employed for surface-catalyzed transformations, adapts to varying assumptions regarding reaction pathways and rate-determining steps, enabling precise fits to experimental data. Similarly, the power-law model, an empirical yet versatile approach, remains highly valued in industrial applications due to its simplicity, reliability, and ease of implementation [36]. These two models are commonly employed to investigate the mechanism of the WGS reaction. Germani et al. [37] investigated WGS kinetics on a thin Pt catalyst layer (0.1 MPa, 473–673 K) under negligible internal diffusion. Their model revealed a nearly zero reaction order for CO, strong inhibition by hydrogen partial pressure, and secondary effects from CO_2 partial pressure, with an activation energy of 76.8 ± 2 kJ·mol^{-1}. A dual-site mechanism was proposed, where Pt adsorbs CO and CeO_2 adsorbs H_2O. The rate-limiting step involves the decomposition of a carboxyl-hydroxyl intermediate at the Pt site, forming CO_2 and H_2.

Despite extensive efforts to clarify the WGS reaction mechanism for catalyst design, consensus on active sites and intermediates remains elusive [38−40]. Currently, two primary mechanisms are recognized: the redox mechanism and the associative mechanism. With the emergence of new catalytic materials and advances in characterization techniques, researchers have developed a new understanding of the WGS reaction mechanism based on these two mechanisms.

The redox mechanism, first proposed by Khan et al. [41] involves two steps: (1) CO is oxidized by surface oxygen to form CO_2 and (2) the catalyst support is oxidized by H_2O, generating H_2. In detail, CO and H_2O are adsorbed onto the catalyst active sites, with H_2O dissociating into O* and H* in steps. CO then reacts with the adjacent O* to form CO_2, and the remaining H* combines to produce hydrogen. The reaction mechanism

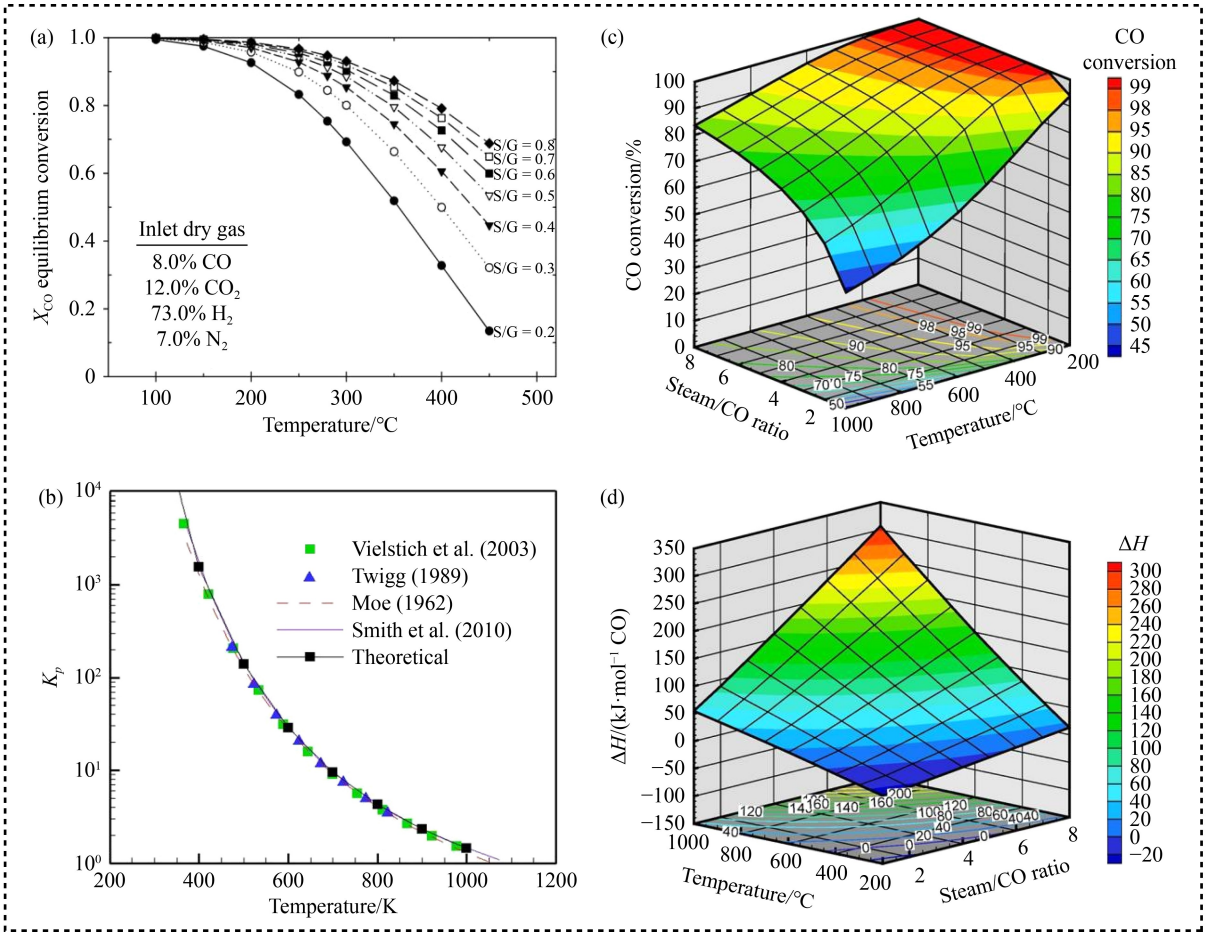

Fig. 2 (a) CO equilibrium conversion of a typical reformer flow during methane steam reforming at different steam to dry gas (S/G) ratios. Reprinted with permission from Ref. [33], copyright 2009, Wiley. (b) Distribution of WGS equilibrium constants. WGS (c) CO conversion and (d) three-dimensional distribution of thermal reactions. Reprinted with permission from Ref. [22], copyright 2019, Elsevier.

can be summarized in six steps, as shown in Eqs. (4)–(9). This mechanism has been further refined and developed in subsequent research. This mechanism primarily applies to HT-WGS catalysts like Fe-Cr oxides and some LT-WGS catalysts supported on reducible carriers (Fig. 3(a)). Boreskov [42] confirmed this mechanism for iron oxide-based catalysts, showing that their reduction and oxidation rates matched the WGS reaction rate. Huang et al. [43] calculated the Fe_3O_4 (111) surface and identified the redox pathway as the most favorable, with COO* desorption as the rate-limiting step. Kalamaras et al. [44] further demonstrated using isotope experiments that Pt/TiO_2 catalysts follow the redox mechanism, where CO adsorbs on Pt, diffuses to the metal-support interface, and reacts with active oxygen to form CO_2.

$$CO + * \leftrightarrow CO* \quad (4)$$

$$H_2O + * \leftrightarrow H_2O* \quad (5)$$

$$H_2O* + * \leftrightarrow OH* + H* \quad (6)$$

$$OH* + * \leftrightarrow O* + H* \quad (7)$$

$$CO* + O* \leftrightarrow CO_2* + * \quad (8)$$

$$H* + H* \leftrightarrow H_2* + * \quad (9)$$

where * represents the catalytic active sites on the surface and X* represents the surface adsorbed species.

The associative mechanism, introduced by Armstrong and Hildtich in 1920 based on Cu-based catalysts, suggests that CO and H_2O adsorb on the catalyst surface and form intermediates (e.g., formate HCOO, carboxyl COOH, and bicarbonate OCOOH), which then dissociate into CO_2 and H_2 (Fig. 3(b)). The related reaction process can be described by Eqs. (10)–(15), where the OH* species generated by the dissociation of CO and H_2O combine to form more complex intermediate species, which then dissociate to produce the final products. Davydov et al. [45] later confirmed the presence of formate species using infrared spectroscopy. Sato et al. [46] further observed that under ambient conditions with water, formates rapidly decompose into CO_2 and H_2. Gokhale et al. [47] through theoretical calculations on the Cu (111) surface, demonstrated that COOH plays a central role in the WGS reaction, while formats serve as a

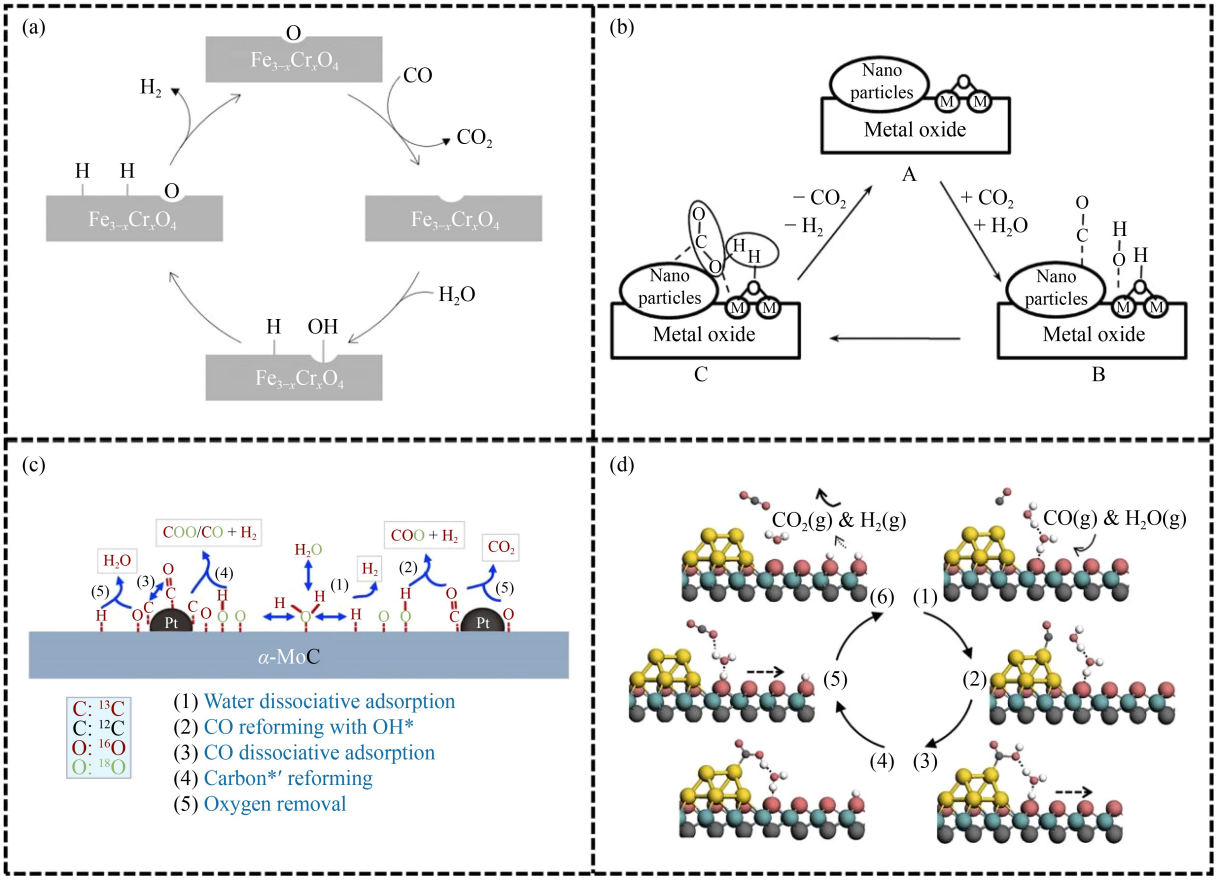

Fig. 3 Schematic diagram of reaction mechanism. (a) Redox mechanism. Reprinted with permission from Ref. [52], copyright 2016, American Chemical Society. (b) Associative mechanism. Reprinted with permission from Ref. [53], copyright 2014, American Chemical Society. (c) Reforming mechanism. Reprinted with permission from Ref. [49], copyright 2021, Nature. (d) Water advancement pathway (WAP) mechanism. Reprinted with permission from Ref. [51], copyright 2021, Elsevier.

stable bystander formed via CO_2 hydrogenation. The carboxyl pathway has consistently shown lower reaction energy in numerous computational studies.

$$CO + * \leftrightarrow CO* \tag{10}$$

$$H_2O + * \leftrightarrow H_2O* \tag{11}$$

$$H_2O* + * \leftrightarrow OH* + H* \tag{12}$$

$$CO* + OH* \leftrightarrow HCOO** \tag{13}$$

$$HCOO** + H_2O \leftrightarrow H_2 + CO_2* + OH* \tag{14}$$

$$CO_2* \leftrightarrow CO_2 + * \tag{15}$$

where * represents the catalytic active sites on the surface, *X** represents the surface adsorbed species, and *X*** represents the surface adsorbate being adsorbed at two active sites.

In recent years, significant advances in catalyst design and mechanistic studies have reshaped the understanding of the WGS reaction mechanism, particularly for LT-WGS. Certain novel materials, such as precious metal catalysts supported on carbon-based or nitride-based carriers, have demonstrated excellent activity in LT-WGS [48−50]. Zhang et al. [49] using isotope labeling techniques, investigated the (Pt_1-Pt_n)/α-MoC catalyst and identified both conventional and unconventional reaction pathways. The conventional pathway involves OH dissociated on α-MoC reacting with CO adsorbed on Pt. The unconventional pathway, however, involves CO dissociating into surface carbon species, which subsequently undergo reforming with H_2O to produce H_2 (Fig. 3(c)). Furthermore, Tian et al. [51] introduced an entirely new reaction mechanism on the Au/TiC_x catalyst. Unlike the traditional pathway where OH/O is generated from H_2O dissociation adsorbs onto the support before desorbing, their findings revealed that H_2O interacts with the support through hydrogen bonding. In this process, CO* adsorbed on Au directly extracts OH from H_2O, forming COOH* and H*. The TiC_x support, with low catalytic activity, merely facilitates the migration of adsorbed H* and its release as H_2 (Fig. 3(d)). These findings demonstrate that the choice of support material can alter the catalytic mechanism, offering new directions for catalyst design and development.

In summary, HT-WGS and LT-WGS differ significantly in thermodynamics, kinetics, and reaction pathways,

which profoundly impact catalyst design strategies, hydrogen production efficiency, and product selectivity. Thermodynamically, the WGS reaction is exothermic, and at elevated temperatures, the equilibrium shifts toward the reverse WGS reaction due to Le Chatelier's principle, thereby reducing hydrogen yield [40,54,55]. Conversely, lower temperatures favor the forward WGS reaction, maximizing hydrogen production but often requiring catalysts with enhanced low-temperature activity to overcome kinetic limitations. Kinetically, higher temperatures accelerate the reaction rate but also promote side reactions such as methanation, coke deposition, and reverse WGS, which lower hydrogen yield and cause catalyst deactivation through sintering or poisoning. Therefore, while HT-WGS offers faster reaction rates, it faces challenges with these side reactions, requiring catalysts with high selectivity and stability. In comparison, LT-WGS, although slower, provides better hydrogen selectivity, fewer side reactions, and improved catalyst stability, making it more efficient for hydrogen production with proper catalyst optimization.

3 Catalyst design for the LT-WGS reaction

An ideal catalyst facilitates the entire WGS reaction cascade, enhancing reactant adsorption, intermediate stabilization, product desorption, and active site regeneration while maintaining structural integrity under prolonged operation [56]. Since WGS is a reaction favorable at low temperatures, designing a low-temperature, highly efficient WGS catalyst can provide both high catalytic activity and thermodynamic advantages, further enabling large-scale hydrogen production through WGS. The hydrogen production efficiency of LT-WGS catalysts reported so far is quite low, and the traditional LT-WGS catalyst $CuO/ZnO/Al_2O_3$ is susceptible to thermal sintering, and its conversion frequency is not high enough [57]. Although noble metal-based shift catalysts exhibit better low-temperature reaction activity, the high content of H_2 in the feed gas can lead to the irreversible over-reduction of the reducible support, leading to rapid catalyst deactivation. In addition, with the growing demand for fuel cells, such as those used in vehicles, more stringent requirements are placed on the performance and low-temperature activity of LT-WGS catalysts. These catalysts not only need to reduce reactor size and significantly increase operating space velocity but must also maintain high activity and stability during frequent start-stop operations.

3.1 Metal/reducible oxide catalysts for the LT-WGS reaction

Reducible supports, also known as active supports, are generally reducible transition metal oxides such as CeO_x [58], TiO_2 [59], MnO_x [60], CoO_x [61], Fe_2O_3 [62], etc. These supports undergo reversible redox transitions via oxygen vacancy formation and annihilation during catalytic cycles, serving as dynamic reservoirs for lattice oxygen. Since the beginning of the 21st century, catalysts supported by reducible supports with metals have remained a focus in LT-WGS research. These catalysts often have noble metals or certain transition metals as active centers, showing remarkable performance improvements in cyclic start-stop and long-term stability tests. However, noble metals are expensive and difficult to activate in water effectively. They are usually added in small quantities to the catalyst to serve as CO adsorption sites, while reducible supports typically act as H_2O decomposition sites. Thus, such catalysts typically consist of three components: the metal for CO adsorption, the support capable of decomposing H_2O, and the metal/support interface.

Commonly used metal components include Au [63], Pt [64], Ir [65], and Ru [66], which exhibit optimal CO adsorption and activation capabilities while suppressing methane formation. During the catalytic reaction process, reducible transition metal oxides such as CeO_2, TiO_2, Fe_2O_3, etc., generate oxygen vacancies on their surfaces under reducing conditions, enabling H_2O adsorption and decomposition. The metal/support interface is essential. Metal particles can enhance the reducibility and oxygen exchange capacity of the support surface, and certain catalysts directly facilitate oxygen vacancy formation at the metal/support interface. In turn, the support can modulate the geometric and electronic configurations of the metal, and their synergy significantly enhances WGS reactivity. Pt/CeO_2, as a catalyst with excellent WGS reaction activity, has been studied for many years [67]. In recent years, many researchers have adopted various methods to improve it, achieving some results. Yuan et al. [68] modified Pt/CeO_2 using support doping and bimetallic alloying, introducing lanthanide ions and 3d transition metals into CeO_2 and Pt, respectively (Fig. 4(a)). They investigated the reaction pathways using *in situ* diffuse reflectance infrared Fourier transform spectroscopy (DRIFTS) and found that $Pt^{\delta+}$ is the active site in Pt/CeO_2. However, in the Pt/CeO_2: Tb catalyst, the formate pathway is dominant, while $PtFe/CeO_2$ is more favorable for the carboxyl pathway, proving that alloying metals to promote CO activation is more beneficial for enhancing WGS reaction activity. However, in actual reactions, its deactivation rate is particularly fast, and CeO_2 is inevitably over-reduced by H_2. Liu et al. [69] designed and constructed an $Au@TiO_{2-x}/ZnO(H\text{-}300)$ catalyst with electronic-metal-support interactions (EMSI), and demonstrated by various *in situ* characterization methods that electron transfer occurs from the TiO_{2-x} overlayer to Au (Fig. 4(b)), establishing dual active sites at the interface: $Au^{\delta-}$ species enhance the

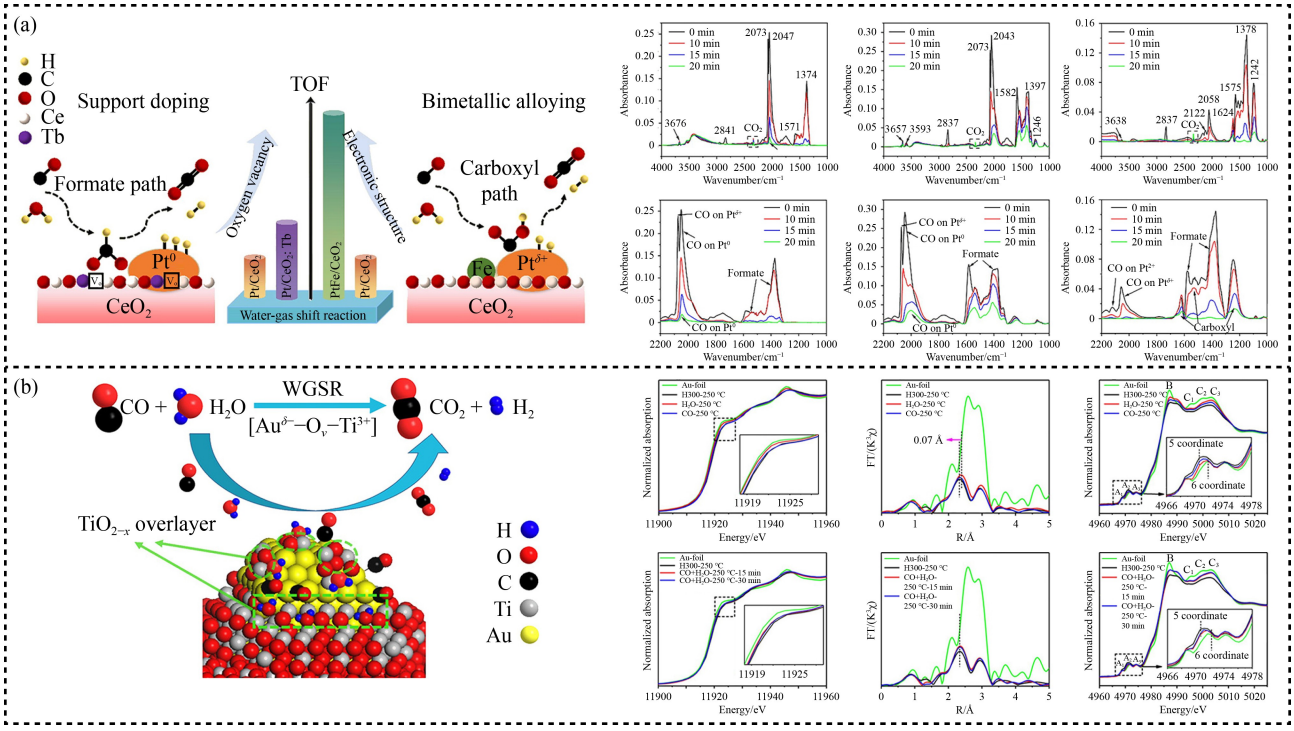

Fig. 4 (a) Pt/CeO_2 modification strategy and *in situ* DRIFTS. Reprinted with permission from Ref. [68], copyright 2021, Elsevier. (b) Schematic of $Au@TiO_{2-x}/ZnO$ reaction mechanism and *in situ* extended X-ray absorption fine structure. Reprinted with permission from Ref. [69], copyright 2019, American Chemical Society.

chemical adsorption of CO, and O_v-Ti^{3+} accelerates the dissociation of H_2O. The reaction mechanism adheres to a redox pathway, resulting in excellent low-temperature catalytic activity. In recent years, there has been increasing research into non-precious metals/reducible supports as alternatives to costly precious metals [70,71]. Yan and colleagues [72] synthesized a uniform block-type Cu/Fe_3O_4 catalyst, which, due to the interaction between Cu and Fe, improved the dispersion of surface CuO, enhanced the adsorption of CO and H_2O, and promoted WGS activity. They further developed a three-component $Cu\text{-}Fe_3O_4\text{-}Al_2O_3$ catalyst to overcome the issue of poor durability. Ning et al. [73] dispersed Cu on rod-shaped CeO_2 and demonstrated that the catalytic activity increased linearly with the Cu content. During this process, Cu forms highly dispersed monolayer or bilayer structures. Controlling the Cu loading within an optimal range facilitates the formation of active sites Cu^{+}-O_v-Ce^{3+}.

3.2 Single-atom metal/oxide catalysts for the LT-WGS reaction

Single-atom catalysis has emerged as a frontier in heterogeneous catalysis, also receiving significant attention in WGS reactions [74]. Single-atom metal/oxide catalysts have been developed on traditional reducible oxide supports by minimizing noble metal loading, with examples including Ru_1/FeO_x [66], Ir_1/FeO_x [65], Pt_1/TiO_2 [75], Pd_1/FeO_x [76], Rh_1/TiO_2 [77], Pt_1/CeO_2 [78], etc. For example, Sun et al. [66] synthesized Ru_1/FeO_x single-atom catalysts using the co-precipitation method and achieved efficient catalytic activity with an exceptionally low loading of 0.18 wt %. According to the hydrogen temperature-programmed reduction results, Ru single atoms promote the reduction of adjacent FeO_x, generating abundant oxygen vacancies that facilitate the dissociation of H_2O. The Ru_1 species can weaken CO adsorption, and collaboratively facilitate the formation of formate or carboxyl intermediates. The dual-site synergy promotes the reaction, demonstrating high performance in the WGS reaction. Ru nanoparticles exhibit a stronger CO adsorption and can promote the dissociation of product H_2 to form highly reactive H*, leading to the formation of methane as a by-product, which significantly reduces the selectivity of the WGS reaction. Remarkably, the single-atom strategy not only generates abundant oxygen vacancies and modulates metal-support interactions to boost WGS reaction activity, but also suppresses parasitic reactions by precisely regulating reactants/products adsorption. Shui et al. [78] prepared a series of Pt_1/CeO_2 catalysts with different metal-support interfaces using atomic layer deposition (ALD) technology, and modified the position and coordination structure of Pt single atoms by adjusting the number of ALD cycles. Through systematic experimental characterization and density functional theory (DFT) simulations, it was confirmed that catalysts with a higher Pt-O coordination number exhibit stronger EMSI, which weakens CO adsorption, promotes the transfer of CO* and the formation of

transition states, resulting in excellent activity in LT-WGS reactions. This method of precisely controlling the EMSI of single-atom catalysts by manipulating single-atom position and coordination environment offers great inspiration for the design and construction of single-atom catalysts.

In the investigation of the active site structure for LT-WGS catalysts, researchers have recognized the importance of additives in improving the catalytic performance of supported nano-catalysts. In 2003, Fu et al. [64] used an alkali-promoted strategy to treat a catalyst containing both Au/Pt nanoparticles and single atoms with NaCN, selectively dissolving the nanoparticles while retaining the single-atom species. The unchanged WGS activity and apparent activation energy indicated that Au/Pt single atoms were the active sites. Subsequently, Pt-based LT-WGS single-atom catalysts have been synthesized on various functional and inert supports, including alumina, zeolites, and carbons [79,80]. For instance, Yang et al. [80] loaded Au onto KLTL-zeolite and mesoporous MCM-41, where the addition of alkali metals Na and K led to the formation of stable Au-$O(OH)_x$ species. This transformation made the previously inactive catalyst highly active. Furthermore, the role of Na additives was further explored in Pt-based single-atom catalysts, where Na stabilized Pt single atoms through oxygen bridge bonds, forming Pt(II)-$O(OH)_x$ species [81]. This structure maintained the catalyst's activity and stability at low temperatures. Regardless of whether the oxide was "active" or "inert", Na additives were found to provide renewable OH species to the support, which played a crucial role in the formation of active sites and led to enhanced catalytic efficiency.

Collectively, these findings highlight the critical roles of both advanced preparation technologies and additives in engineering high-performance single-atom metal/oxide catalysts for the LT-WGS. Despite the persistently lower metal loading in single-atom catalysts (SACs) compared to conventional systems, their space-time yields remain competitive with traditional catalysts. Moving forward, research efforts must prioritize strategies to strategically augment noble metal loading, thereby unlocking their full potential for enhanced catalytic efficiency.

3.3 Metal/carbide or nitride catalysts for the LT-WGS reaction

In addition to traditional oxide supports, researchers are continuously searching for other catalytic materials to develop efficient LT-WGS catalysts. Some transition metal carbides/nitrides (TMCs/TMNs) have been proven to be effective systems. As early as 1973, WC exhibited catalytic performance surpassing that of metal W in a series of surface catalytic reactions, similar to the noble metal Pt. In subsequent research, TMCs have shown catalytic performance close to or even surpassing that of noble metals, and have been widely applied in the WGS reaction [82]. Patt's group was the first to report the efficient catalytic performance of β-Mo_2C in the WGS reaction [83]. At atmospheric pressure and temperatures between 493 and 568 K, its activity was significantly higher than that of the commercial $Cu/ZnO/Al_2O_3$ catalyst, with almost no methanation side reactions and extremely high selectivity. Moon et al. [84] found that the low-valence Mo in β-Mo_2C is oxidized to MoO_3 during reactions with H_2O, leading to deactivation during thermal cycling. Later on, the Co- and Ni-doped bimetallic carbides ($Co_xMo_{1-x}C_y$, $Ni_xMo_{1-x}C_y$) exhibit higher activity (~7 $\mu mol \cdot g_{cat}^{-1} \cdot s^{-1}$ at 473 K) than bare β-Mo_2C but have lower stability [85,86]. Subsequently, researchers explored strategies to enhance their durability and developed a series of metal/β-Mo_2C supported catalysts (Fig. 5(a)). Patt's group was the first to report the efficient catalytic performance of β-Mo_2C in the WGS reaction [83]. The 4% Pt/β-Mo_2C catalyst achieved a high activity of 227 $\mu mol \cdot g_{cat}^{-1} \cdot s^{-1}$ at 513 K, nearly 10 times that of the most active metal/oxide catalyst and 5 times that of bare β-Mo_2C under the same conditions. Following a similar strategy, Pt, Au, and Pd/β-Mo_2C catalysts were synthesized, demonstrating high activity at just 393 K (1.4–1.8 $\mu mol \cdot g_{cat}^{-1} \cdot s^{-1}$), 4–8 times higher than commercial Cu-based catalysts. In contrast, Ni, Cu, and Ag/β-Mo_2C were less active [87,88]. Accordingly, the selection of ad-metal species critically governs catalytic performance, with Pt- and Au-based catalysts exhibiting smaller CO and larger H_2O kinetic orders, indicating CO adsorption as the rate-limiting step in the LT-WGS reaction. Their superior activity is attributed to their ability to maintain high CO surface coverage.

In addition to traditional TMCs, researchers in recent years have also explored new TMCs/TMNs, which show better catalytic promotion for the WGS reaction. Another crystalline phase of molybdenum carbide, α-MoC, shows even better LT-WGS activity and has garnered widespread attention. Yao et al. [48] synthesized the Au/α-MoC catalyst that achieve unprecedented LT-WGS activity, exceeding previous benchmarks by an order of magnitude 423 K. Through experiments such as temperature programmed surface reaction (TPSR), it was proven that the α-MoC surface contains low-temperature H_2O dissociation centers, capable of generating H_2 and OH* species. The Au clusters significantly enhanced the interfacial reaction rate between the adsorbed CO and the hydroxyl groups on the support, which is generally the rate-determining step in the WGS reaction. Building upon this foundation, the research group engineered a (Pt_1-Pt_n)/α-MoC catalyst featuring cooperative Pt nanocluster-single-atom configurations. This innovation addressed dual challenges in Au/α-MoC systems: narrow thermal operating windows and high-temperature deactivation while achieving an activity surge approaching an order of magnitude enhancement [49]. Using isotope

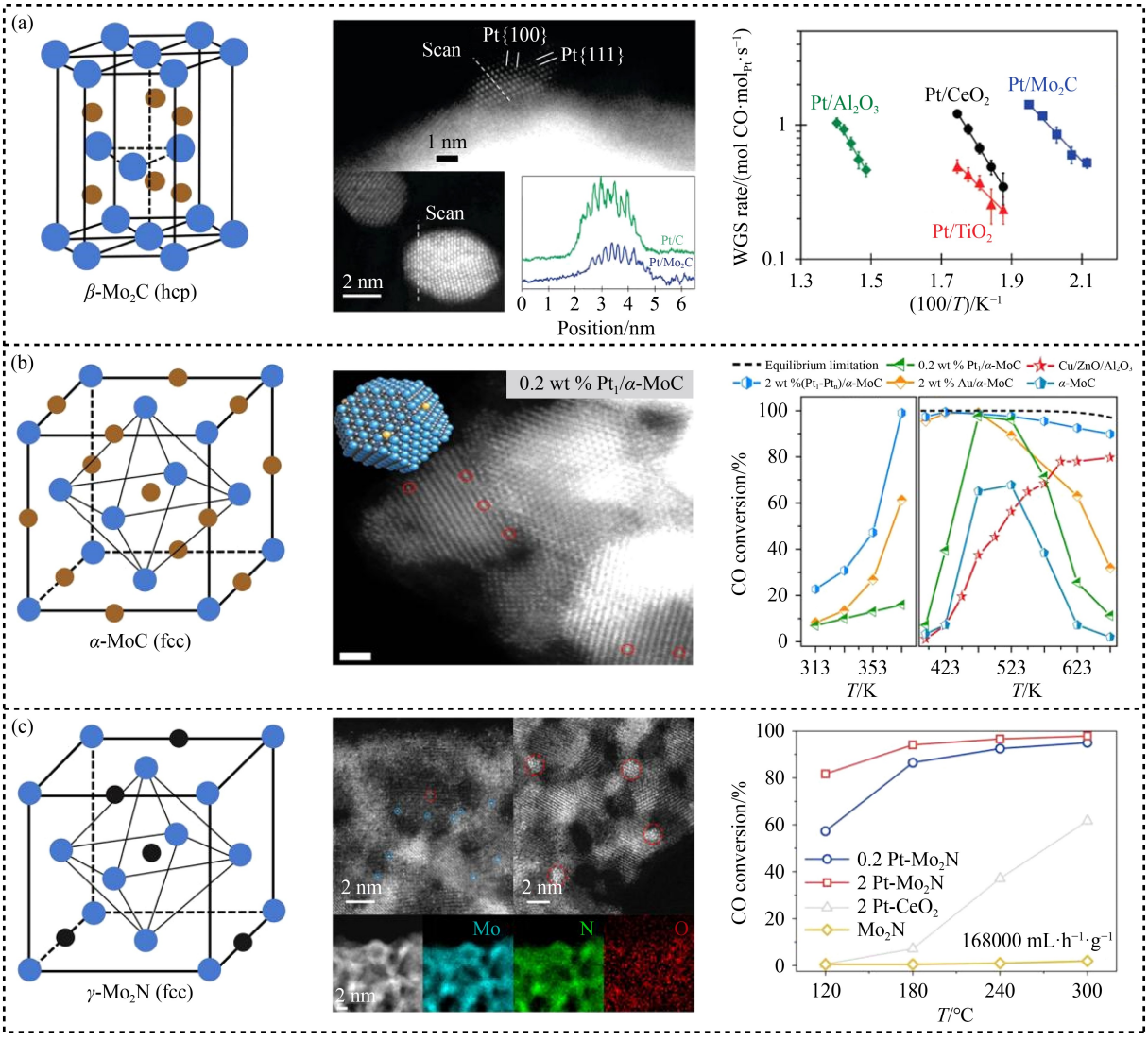

Fig. 5 Cell structure, electron microscopy, and activity diagrams of (a) β-Mo_2C (hcp: hexagonal close-packed). Reprinted with permission from Ref. [89], copyright 2011, American Chemical Society. (b) α-MoC (fcc: face-centered cubic). Reprinted with permission from Ref. [49], copyright 2021, Nature. (c) γ-Mo_2N. Reprinted with permission from Ref. [50], copyright 2020, American Chemical Society.

labeling techniques to investigate the reaction mechanism, it was discovered that, in addition to the conventional pathway involving the reaction of dissociatively adsorbed OH on α-MoC with adsorbed CO on Pt (via redox or associative mechanisms), the (Pt_1-Pt_n)/α-MoC catalyst also features a new pathway where CO dissociates into surface C species and reacts with H_2O to produce H_2 (Fig. 5(b)), providing new insights into the WGS reaction mechanism.

Alongside MoC materials, fcc Mo_2N is also used in LT-WGS reaction studies. Its unique crystal and electronic structure make Mo_2N a valuable support in various catalytic processes, warranting further investigation of its surface reactions. Zhang et al. [50] anchored Pt on the γ-Mo_2N support and observed that the MoO_x species on the support surface with a large number of oxygen vacancies greatly promoted the dissociation of H_2O molecules, generating high stress with γ-Mo_2N, which significantly improved both the reaction activity and stability (Fig. 5(c)). TPSR studies revealed that when CO is not adsorbed on the catalyst surface, neither H_2O nor OH species can dissociate to produce H_2. Theoretical calculations further ruled out the possibility of a redox mechanism for the catalyst, suggesting that COOH could be the reaction intermediate, following an associative mechanism.

3.4 Unconventional metal-based catalysts for the LT-WGS reaction

Carbon materials, as supports, have attracted great interest due to their superior and unique optical, electronic, and mechanical properties. In recent years, various forms of carbon materials as functional catalyst

supports have gained widespread attention from researchers. Zugic et al. [90] reported the promoting effect of Na on the WGS activity of Pt supported on oxygen-free multi-walled carbon nanotubes (CNTs). The author utilized aberration-corrected high-angle annular dark field scanning transmission electron microscopy to investigate the structure and morphology of the catalyst surface, discovering that the addition of Na can stabilize atomically dispersed Pt species. The contribution of the oxidation platinum species (Pt-OH_x) in the Pt 4f signal is higher, and the active sites exist in the form of Pt-Na_x-O_y-$(OH)_z$. This enhanced the activity of the Pt/C catalyst, which originally exhibited almost no activity, to a level comparable to that of highly active platinum catalysts supported on metal oxide carriers. Dongil et al. [91] studied Ni/CeO_2/CNT catalysts for LT-WGS and investigated the effects of different commercial carbon supports on the catalyst. They found that CNTs improved the dispersion of CeO_2, and under these conditions, Ni-CeO_2 exhibited better interactions and higher catalytic activity. Under working conditions, the influence of CO_2 and H_2 was explored, and a slight decrease in activity was observed, with methanation only occurring above 573 K.

In addition to the conventional method of supporting metals on oxide, metal carbide/nitride, and carbon-based materials, researchers have designed catalysts with reverse configurations to better understand the interfacial effect. Diverging from conventional supported configurations, these systems employ metallic matrices as structural scaffolds for oxide nanoparticles, a paradigm shift enabling targeted interface engineering. Yan et al. [92] constructed a stable bulk-nanostructured interface to prepare a CeO_2-Cu reverse catalyst using an aerosol spray method. Through an *in situ* structural transformation, CeO_2 nanoparticles (2–3 nm) are dispersed on bulk Cu, forming a sufficient CeO_2-Cu interface. The enrichment of this interface significantly enhances the activity and stability of WGS. In traditional Cu/CeO_2 catalysts, Cu species are prone to aggregation and sintering, dynamically eroding the Cu-CeO_2 interface and triggering rapid deactivation. Computational studies show that the number of reverse CeO_2-Cu interface sites is four times that of the conventional Cu-CeO_2 catalyst. These sites exhibit strong interactions, leading to a significant improvement in the catalyst's redox properties. The LT-WGS activity is five times higher than that of other Cu catalysts, and the long-term stability tests also demonstrate excellent performance.

To provide a concise yet comprehensive overview of WGS catalyst performance, we have compiled Table 1, which systematically compares the reaction conditions and catalytic metrics of the various systems discussed in this section. This table aims to offer a clear, comparative insight into the performance of different catalysts, highlighting key trends and differences.

4 Innovative WGS reaction processes driven by renewable energy

The WGS reaction is exothermic and is limited by thermodynamic, kinetic, and chemical equilibrium constraints. Conventional thermal catalysis struggles with an irreconcilable trade-off, maximizing equilibrium conversion necessitates low temperatures, while accelerating kinetics demands elevated temperatures. To overcome these limitations, researchers have developed various alternative processes to facilitate the occurrence of the WGS reaction. Building on innovations in LT-WGS catalysts, novel reaction processes driven by renewable energy sources, such as electrochemical and photothermal approaches, have emerged as promising alternatives. These new methods offer more efficient and sustainable reaction conditions by harnessing renewable energy to enhance reaction kinetics and open up new reaction processes and fields, though they do not necessarily achieve conversion rates higher than traditional thermal catalysis.

Electrocatalytic water gas shift (EWGS) reaction. The EWGS process provides a new direction for hydrogen production under low-temperature conditions. The WGS redox reaction is electrochemically decoupled into separate cathodic hydrogen evolution and anodic CO oxidation reactions (Fig. 6(a)). The hydrogen produced at the cathode requires no complex separation and can achieve a purity of 99.99%, presenting excellent prospects for application. The specific reaction process is shown in Eqs. (16)–(18) [100], where CO is oxidized at the anode, and the product CO_2 further reacts with hydroxide ions to form CO_3^{2-}, which is converted into K_2CO_3, thereby preventing pollution caused by CO_2 emissions. Meanwhile, H_2O reduction at the cathode produces H_2. The EWGS reaction typically occurs at ambient temperature and pressure. Compared to conventional water electrolysis, the EWGS reaction has a smaller enthalpy change ($CO(g) + H_2O(l) \rightarrow H_2(g) + CO_2(g)$ $\Delta H_r^\theta = -2.8$ kJ·mol^{-1}), and the initial anode potential (0–0.6 V) is much lower than the theoretical anode potential for water electrolysis (~1.2 V) [103]. Thermodynamically, any type of CO-containing waste gas, such as coke oven gas and syngas, may be suitable for producing high-purity H_2 through this method. In the EWGS reaction, the slow anode CO oxidation is a key factor limiting the overall reaction efficiency [100].

$$\text{Anode}: \ CO + 4OH^- \rightarrow CO_3^{2-} + 2H_2O + 2e^- \quad (16)$$

$$\text{Cathode}: \ 2H_2O + 2e^- \rightarrow H_2 + 2OH^- \quad (17)$$

$$\text{Total}: \ CO + 2OH^- \rightarrow H_2 + CO_3^{2-} \quad (18)$$

Designing and constructing suitable anode catalysts to reduce the overpotential is beneficial for the occurrence

Table 1 Overview of the activity and reaction mechanisms of different types of WGS catalysts

Catalyst	Gas hourly space velocity/ ($mL \cdot h^{-1} \cdot g_{cat.}^{-1}$)	Feed composition	T/K	Mass specific rate/ ($\mu mol_{H_2} \cdot g_{cat.}^{-1} \cdot s^{-1}$)	Ref.
Metal/reducible oxide					
1% Pt/CeO_2:Tb	84000	2% CO + 10% H_2O	473	3.39	[68]
0.01% Pt_1/FeO_x	18000	2% CO + 10% H_2O	573	1.16	[65]
0.5% Pt_1-Na/TiO_2	124200	11% CO + 26% H_2O + 26% H_2 + 7% CO_2	573	3.70	[81]
Au/CeO_2	–	11% CO + 26% H_2O + 26% H_2 + 7% CO_2	523	4.80	[64]
0.5% Au_1/CeO_2 (La doped)	15000 (h^{-1})	11% CO + 26% H_2O + 26% H_2 + 7% CO_2	473	5.10	[93]
Au@TiO_{2-x}/ZnO(H300)	13200	6% CO + 25% H_2O	523	15.98	[69]
Single-atom metal/oxide					
0.01% Ir/FeO_x	18000	2% CO + 10% H_2O	573	1.21	[65]
0.21% Pt (SACs)/CeO_2	168000	2% CO + 10% H_2O	523	2.37	[94]
0.18 Ru/FeO_x	18000	2% CO + 10% H_2O	573	3.81	[66]
0.37% Rh_1/TiO_2	18000	2% CO + 10% H_2O	573	21.94	[77]
1.16 Au/TiO_2 (UV)	124200	11% CO + 26% H_2O + 26% H_2 + 7% CO_2	473	13.90	[95]
PtCe-2	75000	2% CO + 8% H_2O	523	13.31	[78]
0.07% Pt/Al_2O_3-AD	15000	5% CO + 20% H_2O	473	12.80	[96]
0.25% Au-K/KLTL	24840	11% CO + 26% H_2O + 26% H_2 + 7% CO_2	423	0.82	[80]
TMC/TMN supports					
1% Pt/Nb_2CT_xMXene	10000	6.8% CO + 21.9% H_2O + 8.5% CO_2 + 37.4% H_2	573	8.20	[97]
2 wt % Au/α-MoC	90000	11% CO + 26% H_2O + 26% H_2 + 7% CO_2	473	207.69	[48]
2wt % (Pt_1-Pt_n)/α-MoC	743000	11% CO + 26% H_2O + 26% H_2 + 7% CO_2	523	823.99	[49]
0.33% Ir_1/α-MoC	18000	2% CO + 10% H_2O	473	20.46	[98]
2% Pt/γ-Mo_2N	840000	5% CO + 25% H_2O	573	831.00	[50]
Others					
CeO_2/Cu	42000	2% CO + 10% H_2O	573	47.50	[92]
1% Pt_1Na_6/1000-2h-C_N	42000	2% CO + 10% H_2O	523	7.29	[90]
CeO_{2-x}/CoO_{1-x}/Co	168000	2% CO + 10% H_2O	523	720.00	[99]

of EWGS. Wei et al. [104] reported a PdCu alloy nanoparticle catalyst ($Pd_{0.7}$Cu/CNTs) supported on CNTs for anodic CO oxidation. By adjusting the Pd to Cu ratio, the catalyst's reaction activity was optimized. The electrochemical potential for CO oxidation driven at a current density of 100 $mA \cdot cm^{-2}$ significantly decreased to 0.74 V *vs.* RHE, much lower than the potential on Pd/CNTs. At 0.3 V, it achieved a high specific activity of 19.9 $mA \cdot mg_{Pd}^{-1}$, more than 330 times higher than that of pure Pd catalysts. DFT calculations reveal that in the anode CO oxidation process, introducing Cu into Pd weakens the adsorption of CO* and enhances the adsorption of OH* from the solution, thereby optimizing the CO oxidation pathway and significantly lowering the overpotential. Wang et al. [105] utilized gas diffusion electrodes to enhance the local CO concentration near the anode catalyst, effectively addressing the issue of reduced reaction performance caused by the concentration gradient of dissolved CO in the EWGS reaction. The authors precisely designed a series of 2.5Pt-xCu/Fe_2O_3 (x = 0, 2, 5) catalysts using a complex precipitation method to form a unique Pt-O-Cu structure, which effectively improved CO adsorption and OH activation. 2.5Pt-2Cu/Fe_2O_3 exhibited an ultra-low onset potential, optimal specific activity, and excellent mass activity (1.5 $A \cdot mg_{Pt}^{-1}$) in anode CO oxidation, more than 15 times higher than commercial Pt/C. It also exhibited remarkable anti-oxidation performance and demonstrated versatility in accommodating feed gases with any CO concentration, highlighting its broad application potential. Compared to traditional thermal catalytic WGS reactions, EWGS can enhance the reaction equilibrium constant through an electric field, thereby producing high-purity hydrogen gas, with advantages of low energy consumption and high energy conversion efficiency. However, EWGS still requires extra electrical energy input, which raises the cost of industrialization. Moreover, the reaction system is not yet fully developed and remains unstable, posing a key challenge for future industrialization.

Light-driven WGS reaction. Solar energy is widely recognized as the most abundant clean energy source in the world and it is extensively applied in photovoltaic conversion and solar thermal applications. The direct use of solar energy to catalyze WGS can greatly reduce energy consumption, enabling cleaner and more efficient energy conversion. The photocatalytic process utilizes a

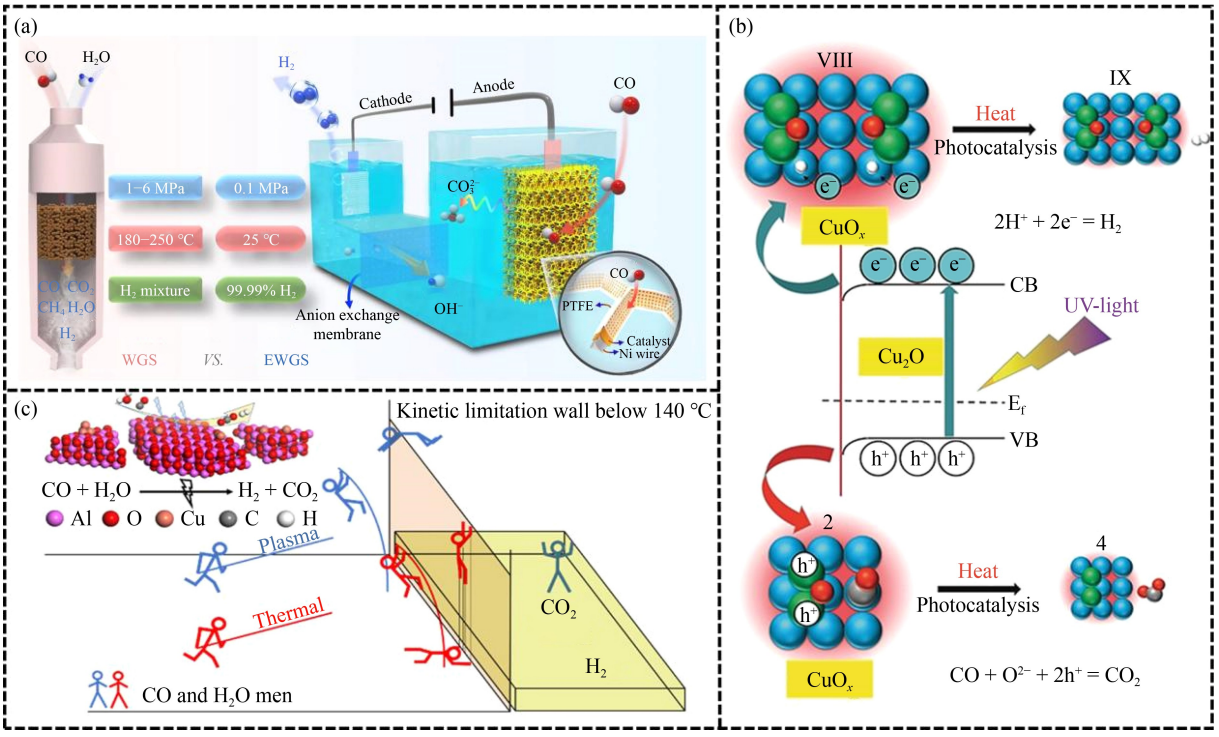

Fig. 6 (a) Schematic diagram of electrocatalytic WGS reaction compared with thermo-catalytic WGS. Reprinted with permission from Ref. [100], copyright 2019, Nature. (b) Schematic diagram of photothermal analysis and photocatalytic decoupling process. Reprinted with permission from Ref. [101], copyright 2019, Wiley. (c) Schematic comparison of plasma-catalyzed WGS with thermo-catalyzed WGS. Reprinted with permission from Ref. [102], copyright 2024, American Chemical Society.

large amount of light energy to initiate and promote chemical reactions [106]. During the reaction, light absorption by catalysts generates electron-hole pairs, which serve as photo-generated charge carriers. These carriers migrate to the catalyst surface, where they interact with adsorbed molecules, facilitating redox reactions such as CO oxidation and hydrogen evolution. Tong et al. [107] designed the $CeO_2/Cu_{1.5}Mn_{1.5}O_4$ catalyst for the photo-thermal WGS reaction and conducted control experiments to investigate the effect of photo-generated carriers on the WGS reaction. The study found that the actual equilibrium constant for the photo-thermal catalyzed WGS reaction greatly exceeded the theoretical equilibrium constant, and its apparent activation energy was significantly reduced by 61% compared to thermal catalysis. This demonstrates the involvement of photo-generated carriers in the reaction process, and injecting these carriers into active sites may induce the transformation of reactant molecules into radicals, thereby lowering the apparent activation energy. Zhao et al. [101] reported a solar-driven WGS reaction on CuO_x/Al_2O_3, using different optical filters to control light exposure during the experiment. They observed that although UV light does not generate heat, it can promote the photocatalytic process, thus validating the coupling effect of photocatalysis and photothermal catalysis in the CuO_x/Al_2O_3 catalyst (Fig. 6(b)). The authors used electron paramagnetic resonance technology and a sacrificial agent to explore the reaction process: UV light drives CO oxidation, creating interfacial oxygen vacancies. With the combined effect of photo-generated carriers and heat, H_2O is reduced, and hydroxyl groups are dissociated at the metal-semiconductor interface, forming a hydrogen bond network that promotes solar-driven H_2 production. Zhao et al. [108] first utilized the local surface plasmon resonance (LSPR) effect in Cu nanoparticle-based catalysts to significantly improve the performance of the WGS reaction. They synthesized copper-based catalysts derived from layered double hydroxide nanosheets, with Cu nanoparticles highly dispersed on an amorphous alumina support. The light-induced LSPR effect of Cu generates hot electrons, which are transferred to adsorbates like H_2O, enhancing the activation of the adsorbates, significantly lowering the operating temperature of the WGS reaction, and improving its activity under mild conditions.

The solar-driven WGS reaction utilizes renewable solar energy, significantly reducing energy consumption and offering an economical approach to hydrogen production. However, its large-scale application faces several challenges, including low energy conversion efficiency, unclear reaction mechanisms, and poor stability. Additionally, environmental factors such as diurnal and seasonal irradiance fluctuations result in intermittent energy availability, hindering its direct substitution for conventional WGS processes. Future research should focus on enhancing solar energy utilization efficiency, elucidating the underlying reaction mechanisms,

developing more stable and efficient photocatalysts, and integrating energy storage systems to improve reliability and scalability.

Plasma-driven WGS reaction. Plasma is regarded as the "fourth state of matter," consisting of neutral substances (atoms and molecules), excited chemicals, free radicals, ions, and high-energy electrons. Plasma can directly activate reactant molecules at the microscopic level through electron collisions, enabling the activation of thermodynamically stable molecules under ambient conditions (Fig. 6(c)). Plasma catalysis can accelerate reaction kinetics under mild conditions, making it widely recognized as a promising alternative to traditional thermal catalytic processes. However, the plasma-driven WGS reaction system is highly complex, including but not limited to plasma discharge, molecular dissociation, ionization and reactions in the gas phase, the effect of the catalyst on plasma discharge, material transport between the gas and solid phases, surface reactions, as well as the light and thermal effects generated by plasma [109]. In simple terms, plasma induces the generation of a large number of high-energy electrons in power plants, activating gas molecules to produce various reactive species such as ions, free radicals, and excited molecules. All species are transported and interact in a multiphase system, with species/molecules adsorbed onto surfaces through adsorption and direct collisions [110]. There is still a lack of investigation into the basic kinetic information of plasma-driven WGS reactions. Notably, the electron temperature in non-thermal plasma (NTP) far exceeds that of heavy particles, leading to non-thermal equilibrium characteristics, traditional thermodynamic theories cannot be used to explore the process, highlighting the need for advanced kinetic models.

Stere et al. [111] compared the use of NTP to drive the WGS reaction under conditions with and without a catalyst. Under catalyst-free conditions, the WGS reaction was tested using a dielectric barrier discharge reactor, and the CO conversion rate was approximately 10%. *In situ* DRIFTS was used to study the reaction process, revealing that NTP can activate H_2O in the gas phase to form hydroxyl species, which in turn drive the reaction. Shen et al. [102] coupled the Cu/γ-Al_2O_3 catalyst with NTP, achieving performance far exceeding that of traditional catalysts at the same temperature of 413 K, with a CO conversion rate of 72.1%, H_2 yield of 67.4%, and energy consumption of only 8.74% MJ·mol^{-1}. Combining DFT calculations and plasma-coupled *in situ* diffuse reflectance Fourier transform spectroscopy, it was shown that the OH radicals generated by NTP react with surface OH* species, thus influencing the redox pathways. Additionally, the OH radicals also react with CO* adsorbed on the catalyst to form COOH*, affecting the carboxylation reaction pathway. This provides new insights into the mechanism of plasma catalysis for the WGS reaction. Xu et al. [112] investigated the catalytic activity and synergistic mechanisms of metal-organic frameworks (MOFs) under NTP conditions for the WGS reaction: under NTP conditions, more unsaturated Cu metal sites in HKUST-1 are available for CO binding, while NTP promotes the dissociation of H_2O, providing OH radicals and preventing H_2O-induced decomposition of HKUST-1, thus improving its stability. This strategy was further applied to various Cu MOFs, demonstrating its general applicability and providing strong evidence for the future practical applications of NTP-driven WGS reactions.

Although considerable progress has been made in plasma-driven WGS reactions in recent years, the design of plasma-related reactors is still limited to the experimental stage, and the scaling-up of the reactors has not been achieved, hindering its industrialization. Furthermore, key challenges, such as limited energy efficiency, the operational complexity of generating stable plasmas at industrial scales, and incomplete insights into reaction mechanisms like plasma-catalyst interactions, continue to hinder the practical deployment of plasma-driven WGS systems. However, ongoing advancements in reactor design, process optimization via machine learning, and deeper mechanistic understanding through in operando diagnostics are paving the way for scalable solutions. These developments hold significant promise for achieving industrial-scale hydrogen production with improved efficiency and cost-effectiveness in the near future.

5 Summary and outlook

The WGS reaction plays a critical role in industrial hydrogen production, with projections indicating that by 2030, approximately 10% of global energy consumption will be associated with this reaction. Significant progress has been made in LT-WGS catalysis over the past few decades, particularly in catalyst design and material innovation. While low-temperature metal/oxide catalysts show promise in improving reaction activity and stability, their initial performance below 473 K remains limited, posing a significant challenge in current research. In contrast, metal/carbide catalysts exhibit excellent low-temperature activity; however, their scalability and industrial applicability have yet to be fully realized. Additionally, emerging catalytic processes such as photocatalysis, electrocatalysis, and plasma catalysis have introduced novel pathways for the WGS reaction, though these technologies still face major challenges related to efficiency, mechanistic understanding, and operational stability. Therefore, future research should focus on the following areas:

(1) Innovative design of highly efficient low-temperature catalysts low-temperature metal/oxide catalysts exhibit poor activity below 473 K due to

insufficient active sites or limited redox properties. Future research should focus on optimizing the catalyst surface structure through strategies such as nano structuring, interface engineering, or the incorporation of co-catalysts to enhance performance at low temperatures. Additionally, exploring novel support materials, such as two-dimensional materials and alloy catalysts, may offer new opportunities to improve low-temperature activity. While metal/carbide (nitride) catalysts demonstrate excellent low-temperature activity, challenges related to large-scale synthesis and industrial application remain. Future studies should focus on improving the scalability, cost-effectiveness, and long-term stability of these catalysts, while evaluating their industrial performance under realistic reaction conditions, particularly in complex atmospheres and at high temperatures.

(2) Efficiency and mechanistic studies of emerging catalytic processes: although emerging catalytic processes such as photocatalysis, electrocatalysis, and plasma catalysis offer innovative approaches for LT-WGS reactions, these technologies still face challenges regarding low efficiency, unclear reaction mechanisms, and poor stability. Future research should prioritize elucidating the fundamental mechanisms behind these processes, optimizing reaction conditions, and improving the stability and efficiency of catalytic systems. Additionally, the development of new photocatalytic and electrocatalytic materials is critical to enhancing the efficiency of these emerging processes.

(3) Interdisciplinary catalyst design and development: with continuous advancements in nanotechnology, material science, and computational chemistry, future research will increasingly rely on interdisciplinary approaches to catalyst design and development. By combining theoretical calculations, experimental studies, and advanced characterization techniques, a deeper understanding of catalyst reaction mechanisms can be gained, thereby accelerating the optimization process. Moreover, integrating intelligent catalyst design and artificial intelligence algorithms is expected to expedite the discovery and optimization of catalysts.

Competing interests The authors declare that they have no competing interests.

Acknowledgements The work was supported by the National Key R&D Program of China (Grant No. 2024YFB4006702), Dalian Science and Technology Talent Innovation Support Program Project (Grant No. 2023RY011), Dalian Science and Technology Innovation Fund Project (Grant No. 2024JJ12CG031), Dalian University of Technology Xinghai Outstanding Young Scholar Program.

References

1. Gunathilake C, Soliman I, Panthi D, Tandler P, Fatani O, Ghulamullah N A, Marasinghe D, Farhath M, Madhujith T, Conrad K, et al. A comprehensive review on hydrogen production, storage, and applications. Chemical Society Reviews, 2024, 53(22): 10900–10969
2. Staffell I, Scamman D, Abad A V, Balcombe P, Dodds P E, Ekins P, Shah N, Ward K R. The role of hydrogen and fuel cells in the global energy system. Energy & Environmental Science, 2019, 12(2): 463–491
3. Wei S J, Sacchi R, Tukker A, Suh S, Steubing B. Future environmental impacts of global hydrogen production. Energy & Environmental Science, 2024, 17(6): 2157–2172
4. Odenweller A, Ueckerdt F, Nemet G, Jensterle M, Luderer G. Probabilistic feasibility space of scaling up green hydrogen supply. Nature Energy, 2022, 7(9): 854–865
5. Aravindan M, Kumar M V, Hariharan V S, Narahari T, Kumar A P, Madhesh K, Kumar P G, Prabakaran R. Fuelling the future: a review of non-renewable hydrogen production and storage techniques. Renewable & Sustainable Energy Reviews, 2023, 188: 113791–113814
6. Liu Z, Jackson G S, Eichhorn B W. Tuning the CO-tolerance of Pt-Fe bimetallic nanoparticle electrocatalysts through architectural control. Energy & Environmental Science, 2011, 4(5): 1900–1903
7. Habashy M M, Ong E S, Abdeldayem O M, Al-Sakkari E G, Rene E R. Food waste: a promising source of sustainable biohydrogen fuel. Trends in Biotechnology, 2021, 39(12): 1274–1288
8. Xu X L, Dong Y, Hu Q W, Si N, Zhang C W. Electrochemical hydrogen storage materials: state-of-the-art and future perspectives. Energy & Fuels, 2024, 38(9): 7579–7613
9. Cheng H, Xia J, Wang M, Wang C, Gui R, Cao X, Zhou T, Zheng X, Chu W, Wu H, et al. Surface anion promotes Pt electrocatalysts with high CO tolerance in fuel-cell performance. Journal of the American Chemical Society, 2022, 144(48): 22018–22025
10. Anetjarvi E, Vakkilainen E, Melin K. Benefits of hybrid production of e-methanol in connection with biomass gasification. Energy, 2023, 276: 127202–127206
11. Giuliano A, Freda C, Catizzone E. Techno-economic assessment of bio-syngas production for methanol synthesis: a focus on the water-gas shift and carbon capture sections. Bioengineering, 2020, 7(3): 70–89
12. Fajin J L C, Cordeiro M N D S. Light alcohols reforming towards renewable hydrogen production on multicomponent catalysts. Renewable & Sustainable Energy Reviews, 2021, 138: 110523–110534
13. Ma Y, Dong X, Wang R, Bin D, Wang Y, Xia Y. Combining water reduction and liquid fuel oxidization by nickel hydroxide for flexible hydrogen production. Energy Storage Materials, 2018, 11: 260–266
14. Bae J, Lee S, Kim S, Oh J, Choi S, Bae M, Kang I, Katikaneni S P. Liquid fuel processing for hydrogen production: a review. International Journal of Hydrogen Energy, 2016, 41(44): 19990–20022
15. Wang H, Harkou E, Constantinou A, Al-Salemc S M, Manos G, Tang J. From photocatalysis to photon-phonon co-driven catalysis for methanol reforming to hydrogen and valuable by-

products. Chemical Society Reviews, 2025, 54(5): 2188–2207
16. Zhang J Y, Shu M, Niu Y X, Yi L, Yi H H, Zhou Y S, Zhao S Z, Tang X L, Gao F Y. Advances in CO catalytic oxidation on typical noble metal catalysts: mechanism, performance, and optimization. Chemical Engineering Journal, 2024, 495: 153523–153539
17. Newsome D S. The water-gas shift reaction. Catalysis Reviews: Science and Engineering, 1980, 21(2): 275–318
18. Rhodes C, Hutchings G J, Ward A M. Water-gas shift reaction: finding the mechanistic boundary. Catalysis Today, 1995, 23(1): 43–58
19. Ratnasamy C, Wagner J P. Water gas shift catalysis. Catalysis Reviews. Science and Engineering, 2009, 51(3): 325–440
20. Flytzani-Stephanopoulos M. Gold atoms stabilized on various supports catalyze the water-gas shift reaction. Accounts of Chemical Research, 2014, 47(3): 783–792
21. Pal D B, Chand R, Upadhyay S N, Mishra P K. Performance of water gas shift reaction catalysts: a review. Renewable & Sustainable Energy Reviews, 2018, 93: 549–565
22. Chen W H, Chen C Y. Water gas shift reaction for hydrogen production and carbon dioxide capture: a review. Applied Energy, 2020, 258: 114078–114103
23. Arregi A, Amutio M, Lopez G, Bilbao J, Olazar M. Evaluation of thermochemical routes for hydrogen production from biomass: a review. Energy Conversion and Management, 2018, 165: 696–719
24. Naseem K, Qin F, Khalid F, Suo G, Zahra T, Chen Z, Javed Z. Essential parts of hydrogen economy: hydrogen production, storage, transportation and application. Renewable & Sustainable Energy Reviews, 2025, 210: 115196–115214
25. Antzaras A N, Lemonidou A A. Recent advances on materials and processes for intensified production of blue hydrogen. Renewable & Sustainable Energy Reviews, 2022, 155: 111917–111953
26. Burns D T, Piccardi G, Sabbatini L. Some people and places important in the history of analytical chemistry in Italy. Microchimica Acta, 2008, 160: 57–87
27. Baraj E, Ciahotny K, Hlincik T. The water gas shift reaction: catalysts and reaction mechanism. Fuel, 2021, 288: 119817–119833
28. Lee D W, Lee M S, Lee J Y, Kim S, Eom H J, Moon D J, Lee K Y. The review of Cr-free Fe-based catalysts for high-temperature water-gas shift reactions. Catalysis Today, 2013, 210: 2–9
29. Ebrahimi P, Kumar A, Khraisheh M. A review of recent advances in water-gas shift catalysis for hydrogen production. Emergent Materials, 2020, 3(6): 881–917
30. Dehimi L, Alioui O, Benguerba Y, Yadav K K, Bhutto J K, Fallatah A M, Shukla T, Alreshidi M A, Balsamo M, Badawi M, et al. Hydrogen production by the water-gas shift reaction: a comprehensive review on catalysts, kinetics, and reaction mechanism. Fuel Processing Technology, 2025, 267: 108163–108182
31. Smith B R J, Loganathan M, Shantha M S. A review of the water gas shift reaction kinetics. International Journal of Chemical Reactor Engineering, 2010, 8(1): 1–32
32. Chein R Y, Yu C T. Thermodynamic equilibrium analysis of water-gas shift reaction using syngases-effect of CO_2 and H_2S contents. Energy, 2017, 141: 1004–1018
33. Mendes D, Mendes A, Madeira L M, Iulianelli A, Sousa J M, Basile A. The water-gas shift reaction: from conventional catalytic systems to Pd-based membrane reactors: a review. Asia-Pacific Journal of Chemical Engineering, 2010, 5(1): 111–137
34. de la Osa A R, De Lucas A, Romero A, Valverde J L, Sanchez P. Kinetic models discrimination for the high pressure WGS reaction over a commercial CoMo catalyst. International Journal of Hydrogen Energy, 2011, 36(16): 9673–9684
35. Li G, Fan M, Lu Y, Glarborg P. Kinetic modeling of carbon monoxide oxidation and water gas shift reaction in supercritical water. Journal of Supercritical Fluids, 2021, 171: 105165–105176
36. Sun J, DesJardins J, Buglass J, Liu K. Noble metal water gas shift catalysis: kinetics study and reactor design. International Journal of Hydrogen Energy, 2005, 30(11): 1259–1264
37. Germani G, Schuurman Y. Water-gas shift reaction kinetics over μ-structured $Pt/CeO_2/Al_2O_3$ catalysts. American Institute of Chemical Engineers, 2006, 52(5): 1806–1813
38. Moazami N, Wyszynski M L, Rahbar K, Tsolakis A, Mahmoudi H. A comprehensive study of kinetics mechanism of Fischer-Tropsch synthesis over cobalt-based catalyst. Chemical Engineering Science, 2017, 171: 32–60
39. Noor T, Qi Y, Chen D. Hydrogen dependence of the reaction mechanism and kinetics of water gas shift reaction on Ni catalyst: experimental and DFT study. Applied Catalysis B: Environmental, 2020, 264: 118430–118439
40. Grenoble D C, Estadt M M, Ollis D F. The chemistry and catalysis of the water gas shift reaction: 1. the kinetics over supported metal-catalysts. Journal of Catalysis, 1981, 67(1): 90–102
41. Khan A, Chen P, Boolchand P, Smirniotis P G. Modified nano-crystalline ferrites for high-temperature WGS membrane reactor applications. Journal of Catalysis, 2008, 253(1): 91–104
42. Boreskov G K. Forms of oxygen bonds on surface of oxidation catalysts. Discussions of the Faraday Society, 1966, 41: 263–276
43. Huang L, Han B, Zhang Q, Fan M, Cheng H. Mechanistic study on water gas shift reaction on the Fe_3O_4 (111) reconstructed surface. Journal of Physical Chemistry C, 2015, 119(52): 28934–28945
44. Kalamaras C M, Gonzalez I D, Navarro R M, Fierro J L G, Efstathiou A M. Effects of reaction temperature and support composition on the mechanism of water-gas shift reaction over supported-Pt catalysts. Journal of Physical Chemistry C, 2011, 115(23): 11595–11610
45. Davydov A A, Boreskov G K, Iurieva T M, Rubene N A. Associative mechanisms of reaction of carbon-monoxide conversion. Doklady Akademii Nauk SSSR, 1977, 236(6): 1402–1405
46. Sato Y, Terada K, Hasegawa S, Miyao T, Naito S. Mechanistic study of water-gas-shift reaction over TiO_2 supported Pt-Re and Pd-Re catalysts. Applied Catalysis A: General, 2005, 296(1): 80–89

47. Gokhale A A, Dumesic J A, Mavrikakis M. On the mechanism of low-temperature water gas shift reaction on copper. Journal of the American Chemical Society, 2008, 130(4): 1402–1414
48. Yao S, Zhang X, Zhou W, Gao R, Xu W, Ye Y, Lin L, Wen X, Liu P, Chen B, et al. Atomic-layered Au clusters on α-MoC as catalysts for the low-temperature water-gas shift reaction. Science, 2017, 357(6349): 389–393
49. Zhang X, Zhang M, Deng Y, Xu M, Artiglia L, Wen W, Gao R, Chen B, Yao S, Zhang X, et al. A stable low-temperature H_2-production catalyst by crowding Pt on α-MoC. Nature, 2021, 589(7842): 396–401
50. Zhang Z S, Fu Q, Xu K, Wang W W, Fu X P, Zheng X S, Wu K, Ma C, Si R, Jia C J, et al. Intrinsically active surface in a Pt/γ-Mo_2N catalyst for the water-gas shift reaction: molybdenum nitride or molybdenum oxide? Journal of the American Chemical Society, 2020, 142(31): 13362–13371
51. Tian H, He Y, Zhao Q, Li J, Shao X, Zhang Z, Huang X, Lu C, Wang K, Jiang Q, et al. Avoiding Sabatier's conflict in bifunctional heterogeneous catalysts for the WGS reaction. Chem, 2021, 7(5): 1271–1283
52. Zhu M, Wachs I E. Resolving the reaction mechanism for H_2 formation from high-temperature water-gas shift by chromium-iron oxide catalysts. ACS Catalysis, 2016, 6(5): 2827–2830
53. Aranifard S, Ammal S C, Heyden A. On the importance of the associative carboxyl mechanism for the water-gas shift reaction at Pt/CeO_2 interface sites. Journal of Physical Chemistry C, 2014, 118(12): 6314–6323
54. Tserpe E, Waugh K C. A microkinetic analysis of the reverse water gas shift reaction. Studies in Surface Science and Catalysis, 1997, 109: 401–416
55. Kalamaras C M, Dionysiou D D, Efstathiou A M. Mechanistic studies of the water-gas shift reaction over Pt/$Ce_xZr_{1-x}O_2$ catalysts: the effect of Pt particle size and Zr dopant. ACS Catalysis, 2012, 2(12): 2729–2742
56. Tao F, Salmeron M. Surface restructuring and predictive design of heterogeneous catalysts. Science, 2024, 386(6724): eadq0102
57. Tikhov S F, Minyukova T P, Reshetnikov S I, Valeev K R, Vernikovskaya N V, Salanov A N, Cherepanova S V, Sadykov V A. Particularities of low-temperature WGSR over ceramometal and oxide catalysts: effect of catalyst particle size. Chemical Engineering Journal, 2019, 374: 405–411
58. Fu X P, Zhao H, Jia C J. Ceria-based supported metal catalysts for the low-temperature water-gas shift reaction. Chemical Communications, 2024, 60(98): 14537–14556
59. Plata J J, Graciani J, Evans J, Rodriguez J A, Fernandez Sanz J. Cu deposited on CeO_x-modified TiO_2 (110): synergistic effects at the metal-oxide interface and the mechanism of the WGS reaction. ACS Catalysis, 2016, 6(7): 4608–4615
60. Szenti I, Efremova A, Kiss J, Sápi A, Ovári L, Halasi G, Haselmann U, Zhang Z L, Morales-Vidal J, Baán K, et al. Pt/MnO interface induced defects for high reverse water gas shift activity. Angewandte Chemie International Edition, 2024, 63(8): e202317374
61. Zhang S, Shan J J, Zhu Y, Frenkel A I, Patlolla A, Huang W, Yoon S J, Wang L, Yoshida H, Takeda S, et al. WGS catalysis and *in situ* studies of CoO_{1-x}, $PtCo_n/Co_3O_4$, and $Pt_mCo_{m'}/CoO_{1-x}$ nanorod catalysts. Journal of the American Chemical Society, 2013, 135(22): 8283–8293
62. Chen Y, Lin J, Li L, Qiao B, Liu J, Su Y, Wang X. Identifying size effects of Pt as single atoms and nanoparticles supported on FeO_x for the water-gas shift reaction. ACS Catalysis, 2018, 8(2): 859–868
63. Abdel-Mageed A M, Kučerová G, Bansmann J, Behm R J. Active Au species during the low-temperature water gas shift reaction on Au/CeO_2: a time-resolved operando XAS and DRIFTS study. ACS Catalysis, 2017, 7(10): 6471–6484
64. Fu Q, Saltsburg H, Flytzani-Stephanopoulos M. Active nonmetallic Au and Pt species on ceria-based water-gas shift catalysts. Science, 2003, 301(5635): 935–938
65. Lin J, Wang A, Qiao B, Liu X, Yang X, Wang X, Liang J, Li J, Liu J, Zhang T. Remarkable performance of Ir_1/FeO_x single-atom catalyst in water gas shift reaction. Journal of the American Chemical Society, 2013, 135(41): 15314–15317
66. Sun L, Cao L, Su Y, Wang C, Lin J, Wang X. Ru_1/FeO_x single-atom catalyst with dual active sites for water gas shift reaction without methanation. Applied Catalysis B: Environment and Energy, 2022, 318: 121841–121853
67. Li Y, Kottwitz M, Vincent J L, Enright M J, Liu Z, Zhang L, Huang J, Senanayake S D, Yang W C D, Crozier P A, et al. Dynamic structure of active sites in ceria-supported Pt catalysts for the water gas shift reaction. Nature Communications, 2021, 12(1): 914–923
68. Yuan K, Sun X C, Yin H J, Zhou L, Liu H C, Yan C H, Zhang Y W. Boosting the water gas shift reaction on Pt/CeO_2-based nanocatalysts by compositional modification: support doping versus bimetallic alloying. Journal of Energy Chemistry, 2022, 67: 241–249
69. Liu N, Xu M, Yang Y, Zhang S, Zhang J, Wang W, Zheng L, Hong S, Au Wei M. δ^--O_v-Ti^{3+} interfacial site: catalytic active center toward low-temperature water gas shift reaction. ACS Catalysis, 2019, 9(4): 2707–2717
70. Shen X, Li Z, Xu J, Li W, Tao Y, Ran J, Yang Z, Sun K, Yao S, Wu Z, et al. Upgrading the low temperature water gas shift reaction by integrating plasma with a CuO_x/CeO_2 catalyst. Journal of Catalysis, 2023, 421: 324–331
71. Ilieva L, Ivanov I, Sobczak J W, Lisowski W, Karashanova D, Kaszkur Z, Petrova P, Tabakova T. Effect of support preparation method on water-gas shift activity of copper-based catalysts. International Journal of Hydrogen Energy, 2022, 47(97): 41268–41278
72. Yan H, Qin X T, Yin Y, Teng Y F, Jin Z, Jia C J. Promoted Cu-Fe_3O_4 catalysts for low-temperature water gas shift reaction: optimization of Cu content. Applied Catalysis B: Environmental, 2018, 226: 182–193
73. Ning J, Zhou Y, Chen A, Li Y, Miao S, Shen W. Dispersion of copper on ceria for the low-temperature water-gas shift reaction. Catalysis Today, 2020, 357: 460–467
74. Shui Z, Jiang G, Zhao M, Yang Z, Li G, Hao Z. Recent advances in atomically dispersed metal catalysts for low-temperature water-gas shift reaction. Current Opinion in Chemical Engineering, 2023, 41: 100929–100940
75. Ammal S C, Heyden A. Titania-supported single-atom platinum

catalyst for water-gas shift reaction. Chemieingenieurtechnik, 2017, 89(10): 1343–1349

76. Sun X, Lin J, Zhou Y, Li L, Su Y, Wang X, Zhang T. FeO_x supported single-atom Pd bifunctional catalyst for water gas shift reaction. American Institute of Chemical Engineers, 2017, 63(9): 4022–4031
77. Guan H, Lin J, Qiao B, Miao S, Wang A Q, Wang X, Zhang T. Enhanced performance of Rh_1/TiO_2 catalyst without methanation in water-gas shift reaction. American Institute of Chemical Engineers, 2017, 63(6): 2081–2088
78. Shui Z, Zhang F, Yang H, Zhao M, Zhao Z, Li G, Wei Z, Jiang G, Zhang Z, Hao Z. Tailoring the electronic metal-support interaction of single-atom platinum catalysts for boosting water-gas shift reaction. Advanced Functional Materials, 2025, 35(8): 2415774
79. Cui Z, Song S, Liu H, Zhang Y, Gao F, Ding T, Tian Y, Fan X, Li X. Synergistic effect of Cu^+ single atoms and Cu nanoparticles supported on alumina boosting water-gas shift reaction. Applied Catalysis B: Environment and Energy, 2022, 313: 121468–121475
80. Yang M, Li S, Wang Y, Herron J A, Xu Y, Allard L F, Lee S, Huang J, Mavrikakis M, Flytzani-Stephanopoulos M. Catalytically active Au-$O(OH)_x$-species stabilized by alkali ions on zeolites and mesoporous oxides. Science, 2014, 346(6216): 1498–1501
81. Yang M, Liu J, Lee S, Zugic B, Huang J, Allard L F, Flytzani-Stephanopoulos M. A common single-site Pt(II)-$O(OH)_x$-species stabilized by sodium on “active” and “inert” supports catalyzes the water-gas shift reaction. Journal of the American Chemical Society, 2015, 137(10): 3470–3473
82. Levy R B, Boudart M. Platinum-like behavior of tungsten carbide in surface catalysis. Science, 1973, 181(4099): 547–549
83. Patt J, Moon D J, Phillips C, Thompson L. Molybdenum carbide catalysts for water-gas shift. Catalysis Letters, 2000, 65(4): 193–195
84. Moon D J, Ryu J W. Molybdenum carbide water-gas shift catalyst for fuel cell-powered vehicles applications. Catalysis Letters, 2004, 92(1/2): 17–24
85. Nagai M, Matsuda K. Low-temperature water-gas shift reaction over cobalt-molybdenum carbide catalyst. Journal of Catalysis, 2006, 238(2): 489–496
86. Nagai M, Zahidul A M, Matsuda K. Nano-structured nickel-molybdenum carbide catalyst for low-temperature water-gas shift reaction. Applied Catalysis A: General, 2006, 313(2): 137–145
87. Sabnis K D, Cui Y, Akatay M C, Shekhar M, Lee W S, Miller J T, Delgass W N, Ribeiro F H. Water-gas shift catalysis over transition metals supported on molybdenum carbide. Journal of Catalysis, 2015, 331: 162–171
88. Sabnis K D, Akatay M C, Cui Y, Sollberger F G, Stach E A, Miller J T, Delgass W N, Ribeiro F H. Probing the active sites for water-gas shift over Pt/molybdenum carbide using multi-walled carbon nanotubes. Journal of Catalysis, 2015, 330: 442–451
89. Thompson L T, Schaidle J, Schweitzer N. High activity carbide supported catalysts for water gas shift. Journal of the American Chemical Society, 2011, 133(8): 2378–2381
90. Zugic B, Zhang S, Bell D C, Tao F, Flytzani-Stephanopoulos M. Probing the low-temperature water-gas shift activity of alkali-promoted platinum catalysts stabilized on carbon supports. Journal of the American Chemical Society, 2014, 136(8): 3238–3245
91. Dongil A B, Pastor-Perez L, Escalona N, Sepulveda-Escribano A. Carbon nanotube-supported Ni-CeO_2 catalysts. Effect of the support on the catalytic performance in the low-temperature WGS reaction. Carbon, 2016, 101: 296–304
92. Yan H, Yang C, Shao W P, Cai L H, Wang W W, Jin Z, Jia C J. Construction of stabilized bulk-nano interfaces for highly promoted inverse CeO_2/Cu catalyst. Nature Communications, 2019, 10: 3470–3480
93. Fu Q, Deng W L, Saltsburg H, Flytzani-Stephanopoulos M. Activity and stability of low-content gold-cerium oxide catalysts for the water-gas shift reaction. Applied Catalysis B: Environmental, 2005, 56: 57–68
94. Yuan K, Guo Y, Lin Q L, Huang L, Ren J T, Liu H C, Yan C H, Zhang Y W. Size effect-tuned water gas shift reaction activity and pathway on ceria supported platinum catalysts. Journal of Catalysis, 2021, 394: 121–130
95. Yang M, Allard L F, Flytzani-Stephanopoulos M. Atomically dispersed Au-$(OH)_x$ species bound on titania catalyze the low-temperature water-gas shift reaction. Journal of the American Chemical Society, 2013, 135(10): 3768–3771
96. Chen T, Chen J, Wu J, Song W, Hu S, Feng X, Chen Z, Yuan E, Ji W, Au C T. Atomic-layer-deposition derived Pt subnano clusters on the (110) facet of hexagonal Al_2O_3 plates: efficient for formic acid decomposition and water gas shift. ACS Catalysis, 2023, 13(2): 887–901
97. Li Z, Cui Y, Wu Z, Milligan C, Zhou L, Mitchell G, Xu B, Shi E, Miller J T, Ribeiro F H, et al. Reactive metal-support interactions at moderate temperature in two-dimensional niobium-carbide-supported platinum catalysts. Nature Catalysis, 2018, 1(5): 349–355
98. Sun L, Xu J, Liu X, Qiao B, Li L, Ren Y, Wan Q, Lin J, Lin S, Wang X, et al. High-efficiency water gas shift reaction catalysis on α-MoC promoted by single-atom Ir species. ACS Catalysis, 2021, 11(10): 5942–5950
99. Fu X P, Wu C P, Wang W W, Jin Z, Liu J C, Ma C, Jia C J. Boosting reactivity of water-gas shift reaction by synergistic function over CeO_{2-x}/CoO_{1-x}/Co dual interfacial structures. Nature Communications, 2023, 14(1): 6851–6862
100. Cui X, Su H Y, Chen R, Yu L, Dong J, Ma C, Wang S, Li J, Yang F, Xiao J, et al. Room-temperature electrochemical water-gas shift reaction for high purity hydrogen production. Nature Communications, 2019, 10: 86–94
101. Zhao L, Qi Y, Song L, Ning S, Ouyang S, Xu H, Ye J. Solar-driven water-gas shift reaction over CuO_x/Al_2O_3 with 1.1% of light-to-energy storage. Angewandte Chemie International Edition, 2019, 58(23): 7708–7712
102. Shen X, Craven M, Xu J, Wang Y, Li Z, Wang W, Yao S, Wu Z, Jiang N, Zhou X,et al. Unveiling the mechanism of plasma-catalytic low-temperature water-gas shift reaction over Cu/γ-Al_2O_3 catalysts. JACS Au, 2024, 4(8): 3228–3237

103. Wang S, Zhou C, Shu G, Cao Y, Fan L, Song L, Ma K, Yue H. Insights into the effects of Pt and PtO_x site for electrocatalytic water gas shift reaction via altering supports and calcinated temperatures. International Journal of Hydrogen Energy, 2023, 48(64): 24730–24741
104. Wei H, Liu H, Yu L, Zhang M, Zhang Y, Fan J, Cui X, Deng D. Alloying Pd with Cu boosts hydrogen production via room-temperature electrochemical water-gas shift reaction. Nano Energy, 2022, 102: 107704–107711
105. Wang S, Zhou C, Cao Y, Song L, Zheng L, Ma K, Yue H. Pt-O-Cu anchored on Fe_2O_3 boosting electrochemical water-gas shift reaction for highly efficient H_2 generation. Journal of Catalysis, 2023, 417: 98–108
106. Li Y, Li R, Li Z, Xu Y, Yuan H, Ouyang S, Zhang T. Recent advances in photothermal CO_x conversion. Solar RRL, 2022, 6(10): 2200493–2200503
107. Tong Y, Song L, Ning S, Ouyang S, Ye J. Photocarriers-enhanced photothermocatalysis of water-gas shift reaction under H_2-rich and low-temperature condition over $CeO_2/Cu_{1.5}Mn_{1.5}O_4$ catalyst. Applied Catalysis B: Environmental, 2021, 298: 120551–120561
108. Zhao J, Bai Y, Li Z, Liu J, Wang W, Wang P, Yang B, Shi R, Waterhouse G I N, Wen X D, et al. Plasmonic Cu nanoparticles for the low-temperature photo-driven water-gas shift reaction. Angewandte Chemie International Edition, 2023, 62: e202219299
109. Chen H, Mu Y, Xu S, Xu S, Hardacre C, Fan X. Recent advances in non-thermal plasma (NTP) catalysis towards C1 chemistry. Chinese Journal of Chemical Engineering, 2020, 28(8): 2010–2021
110. Whitehead J C. Plasma-catalysis: the known knowns, the known unknowns and the unknown unknowns. Journal of Physics D: Applied Physics, 2016, 49(24): 243001–243025
111. Stere C E, Anderson J A, Chansai S, Delgado J J, Goguet A, Graham W G, Hardacre C, Taylor S F R, Tu X, Wang Z, et al. Non-thermal plasma activation of gold-based catalysts for low-temperature water-gas shift catalysis. Angewandte Chemie International Edition, 2017, 56(20): 5579–5583
112. Xu S, Chansai S, Stere C, Inceesungvorn B, Goguet A, Wangkawong K, Taylor S F R, Al-Janabi N, Hardacre C, Martin P A, et al. Sustaining metal-organic frameworks for water-gas shift catalysis by non-thermal plasma. Nature Catalysis, 2019, 2(2): 142–148